VACUUM PERFORMANCES AND LESSONS FOR 2012

V. Baglin, G. Bregliozzi, J.M. Jimenez and G. Lanza CERN, Geneva, Switzerland

Abstract

During the LHC run 2011, a tremendous progress has been made towards the machine operation with design parameters. In the same time, the run confirmed the sensitivity of the beam vacuum system to the machine parameters. As expected, a successful scrubbing period allowed mitigating the effects of the electron cloud giving room to an entire filling of the ring with 50 ns beams. In parallel issues such as the impact of the beam screen regulation, pressures spikes and local outgassing were observed during the year. On-line mitigations and immediate compensatory measures implemented during the winter technical stop are reviewed together with their efficiencies. The expected limitations while waiting for LS1 consolidation or when running with 25 ns beams are addressed. Lessons for 2012 are discussed.

INTRODUCTION

The LHC vacuum system is designed to overcome the effects induced by the beams and particularly protons beams [1]. According to the LHC baseline, the vacuum system is designed to operate with ultimate beams [2]. Table 1 summarises the main machine parameters relevant for the vacuum system. In this table, the beam parameters achieved at the end of the 2011 run are compared to the injection, nominal and ultimate LHC parameters.

Table 1: Summary of the main LHC parameters relevant for the vacuum system [2]

	2011	Injection	Nominal	Ultimate
Energy (TeV)	3.5	0.45	7	
Beam current (mA)	362	584		860
Number of protons per bunch	$1.45\ 10^{11}$	$1.15\ 10^{11}$		$1.7\ 10^{11}$
Number of bunch	1380	2808		
Bunch spacing (ns)	50	25		
Critical energy (eV)	5.5	0.01	44	44
Photon flux (ph/m/s)	$3\ 10^{16}$	$6\ 10^{15}$	$1\ 10^{17}$	$1.5\ 10^{17}$
SR power (W/m)	0.01	0	0.22	0.33

When circulating in the LHC arcs, the protons beams produce synchrotron radiation (SR) emitted in the bending magnet beampipes. At injection, the SR spectrum is in the very low energy part below a few tenth of eV. Therefore, only weakly bound molecules can be desorbed under this SR irradiation. Moreover, the photon flux being so small that it makes the photon stimulated desorption hardly observable at injection energy. At flat top, the SR spectrum extends up to the keV range. In this case, weakly bound and tightly bound molecules which are desorbed under photon irradiation are released. No matter the machine parameters, this source of gas will be always present during the LHC lifetime. In the cryogenic arcs of the LHC, the vacuum level is driven by the acceptable power loss in the cold mass due to nuclear scattering onto the residual gas. The design beam lifetime of 100 h, *i.e.* 10^{-8} mbar H_2 equivalent, fulfil this criterion. In consequence, appropriate surface cleanliness and pumping systems provided by perforated beams screens are required to reach the vacuum performances [3].

In the LHC, an electron cloud builds-up induced by the closely spaced and dense proton beams. The interaction of this cloud with the vacuum surroundings results in an electron stimulated molecular desorption. The cloud intensity is a strong function of the maximum secondary electron yield, δ_{max}, of the vacuum chamber walls. In the LHC, the multipacting thresholds have been estimated and depend mainly of the bunch spacing and on the presence of a magnetic field. Recent estimations for 3.5 TeV beams indicate that multipacting thresholds at 25 ns are in the range $1.2 < \delta_{max} < 1.4$. Table 2 gives the multipacting levels for the current LHC operation [4]. A weak dependence with beam energy up to 7 TeV is expected.

Table 2: Multipacting thresholds for current LHC operation [4]

Bunch spacing	Magnetic field	450 GeV	3.5 TeV
50 ns	no	1.7	1.7
	dipole	2.2	2.1
25 ns	no	1.3	1.2
	dipole	1.5	1.4

Since most of the technical materials have a δ_{max} in the range of 2 or above, a surface processing of the LHC vacuum chambers is required to fulfil the vacuum performances. For these reasons, most of the room temperature elements of the machine, including the experimental beampipes, but with the exception of kickers, collimators, BI equipments and some vacuum modules, are coated with Non Evaporable Getter (NEG) coatings made of TiZrV material. Beside its huge pumping performances when applied on large surfaces after vacuum activation, this coating has a very low δ_{max} of 1.1 in a way that multipacting is fully excluded with such materials in the LHC. On the other hand, uncoated areas operating at room temperature or at cryogenic temperature, requires a processing of the surface to reduce δ_{max} below the multipacting threshold *i.e.* beam scrubbing is required. In the LHC, the baseline is to scrub the

vacuum chamber wall under electron bombardment which graphitise the near surface thereby reducing the δ_{max} [5].

Among others, proton storage rings with large circulating beam current must be designed to cope with the so-called "ion induced pressure instability" known from previous experience with the CERN Intersecting Storage Ring (ISR) [6]. The optimisation of the local pumping speed and the local cleanliness of vacuum surfaces are essential ingredients to keep the vacuum stable. In the LHC arcs, the beam screen's perforation associated to the operation with a surface exempt of physisorbed gas guaranty vacuum stability. In the LHC room temperature parts, the combination of the NEG coating cleanliness with its huge pumping speed added to the sputter ion pumps ensure the vacuum stability [7,8].

In this paper, the vacuum observations done during LHC 2011 run are described together with the observation of unexpected pressure rises.

DYNAMICS EFFECTS

Synchrotron Radiation

The first observation of pressure increase of a few 10^{-10} mbar stimulated by SR was already observed with 3.5 TeV beams and reported in summer 2010. During the energy ramping, a pressure increase is seen above 2.5 TeV which corresponds to a photon critical energy of 2 eV. In 2011, the maximum pressure increase due to SR was in the range of 10^{-8} mbar and drops during the year by about two orders of magnitude, as predicted. Figure 1 shows a typical dynamic pressure increase expressed in mbar/A as a function of the accumulated photon dose [9]. The pressure measurement was performed at the arc extremities at the level of the cold/warm transitions. It must be stressed that no pressure increase, due to SR, larger than 5 10^{-9} mbar was observed inside the arcs. The dynamic pressure, which is proportional to the photodesorption yield, reduces with photon dose. The initial yield is estimated to be ~ 10^{-2} molecules/photon. The initial value and the behaviour with photon dose are typical and in agreement with published data [10].

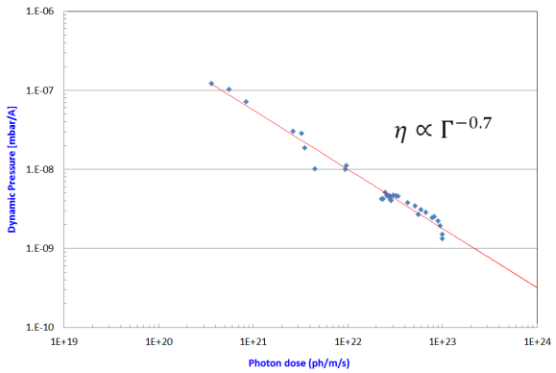

Figure 1: Dynamic pressure increase in mbar/A observed at the LHC arcs extremities as a function of the photon dose.

In 2012, beam conditioning will still be observed reducing further the pressure down to a few 10^{-10} mbar. After LS1, when LHC will operate with design energy, it is estimated that the photodesorption yield will increase by a factor 200 bringing back the pressure in the 10^{-8} mbar range. However, since a nominal LHC year accounts to a photon dose of 10^{24} ph/m, further beam conditioning is expected which will, as stated in the introduction, guaranty a beam lifetime larger than 100 h.

Electron Cloud

The first vacuum observations of electron cloud were already done in 2010 with 150 and 50 ns beams. In 2011, a scrubbing run with 50 ns beams was held together with machine development periods with 25 ns beams [11,12,13].

The scrubbing run held in April 2011 was performed with 50 ns beams with nominal bunch population. At the end of the period, a total of 1020 bunches per beam could be circulated at 450 GeV in the machine. During this period, the heat load measured in the arcs was decreasing with time with a maximum value of ~ 0.05 W/m [14]. Figure 2 shows the dynamic pressure due to electron cloud observed at the cold/warm transitions of the standalone magnets and at NEG-NEG transitions as a function of beam time. After about 30 h of operation, the pressure increase at both locations was reduced by one order of magnitude due to the simultaneous actions of beam conditioning and beam scrubbing. During this period, the reduction of δ_{max} is estimated to be from 1.9 to 1.7 [4].

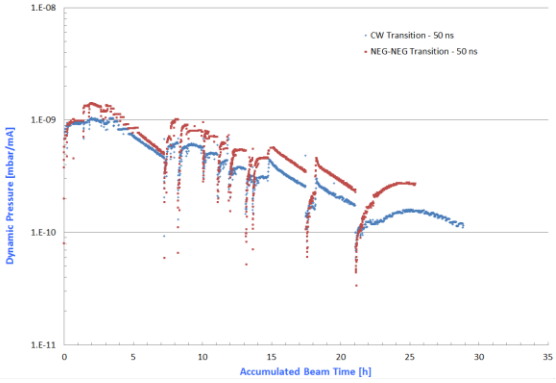

Figure 2: Dynamic pressures increase due to electron cloud observed at the stand alone magnets extremities and NEG-NEG transitions with 50 ns beams as a function of beam time.

The pressure increase, P, due to electron cloud is expressed by (1) with $\eta_{electrons}$ the electron desorption yield, $\Gamma_{electrons}$ the electron flux and S the pumping speed.

$$P = \frac{\eta_{electrons}\dot{\Gamma}_{electrons}}{S} \quad (1)$$

This equation illustrates that the reduction of pressure is due to the decrease of the electron desorption yield under conditioning but also to the decrease of the electron flux to the vacuum chamber wall under beam scrubbing. Figure 3 gives the reduction of the electron desorption yield as a function of δ_{max} for unbaked Cu [15]. Further beam scrubbing performed during the run with reduction of δ_{max} is accompanied by a decrease of the electron

desorption yield *i.e.* beam conditioning. At the end of the 2011 run, δ_{max} in field free regions is estimated to be 1.4 [4]. As seen from Table 2, the field free areas will need further beam scrubbing to operate below the multipacting threshold with 25 ns beams. On the other hand, operation with 50 ns beams can be done without further scrubbing.

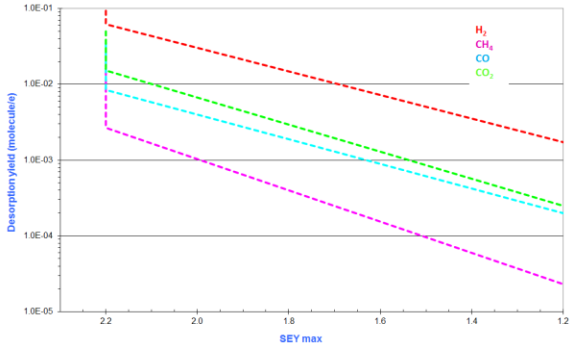

Figure 3: Electron desorption yields for unbaked Cu as a function of δ_{max}.

During MDs with 25 ns beams, significant heat load up to ~ 0.5-1 W/m where observed in the LHC arcs [16]. During this period, the number of bunches was 2100/1020 in B1 and B2 respectively *i.e.* B1 in the LHC machine was almost full. The amount of bunches in B2 was limited by beam induced pressure rise at the level of kickers. Figure 4 shows the pressure rise measured in field free areas at cold/warm transitions and at NEG to NEG transitions. Despite the measurements are made in field free areas, which, as shown previously in Figure 2, have been previously scrubbed during the year, a factor of 50 is noted between the cold/warm and NEG-NEG transitions. However, for the baked system (NEG-NEG transition) there is a clear indication of pre-scrubbing with 50 ns beams. Since the scrubbing efficiency must be the same for the two types of transitions, the observed pressure rise at the level of the cold/warm transition is due to the desorbed gas from the cold system indicating that the cold systems are not fully scrubbed. The observation of this gas load is in agreement with the large heat load dissipated in the cold systems with 25 ns beams. The pressure difference between the two locations is also in qualitative agreement with the different multipacting thresholds and with the fact that the electron flux are larger in field free areas than field regions in such a way that field free areas scrub faster than field regions. This is consistent with estimations of δ_{max} in field free and dipole areas of the LHC [4].

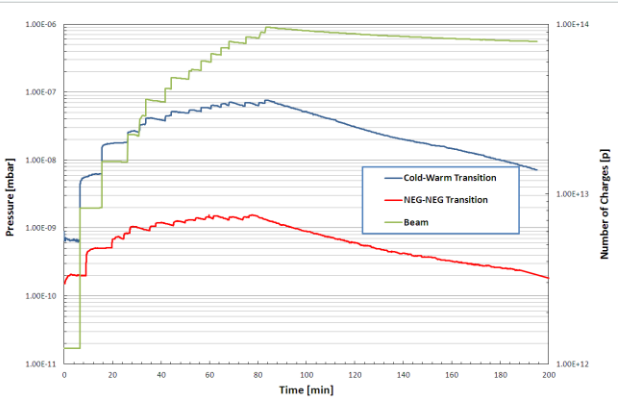

Figure 4: Pressure rise observed with 25 ns beams at the level of cold/warm and NEG-NEG transitions.

Figure 5 gives the overview of the year 2011. The average pressure measured in the Long Straight Sections (LSS) 1, 2, 5 and 8 (blue curve) *i.e.* in the vicinity of the LHC experiments and the average pressure measured at standalone magnets (green curve). The red curve shows the number of proton per bunch which increased from 9 to 14.5 10^{10}. Labels indicating the main events (scrubbing run, number of bunches, etc.) are also shown. Thanks to the scrubbing and beam conditioning of the vacuum system, the average pressures, shown on a log scale, decreased during the year in the range 10^{-9} mbar while pushing the LHC performances.

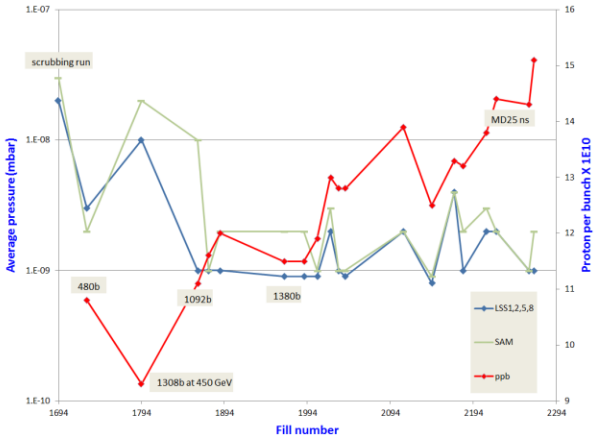

Figure 5: Overview of average pressures during the year 2011.

Dealing with beam screens

After the scrubbing run, the surface coverage of physisorbed gas onto the beam screen was increased due to the stimulated gas desorption. During the beam injection, the image current onto the beam screen raised therefore the He flow inside the beam screens capillary need to be increased. Unfortunately, for some beams screens, particularly those of the Inner Triplets and D1 magnets, the control loops were not fully optimised and, as expected, gas transients appeared [17]. Figure 6 gives an example of such transients. Pressure spikes up to 10^{-6} mbar are observed for temperature oscillations in the

13-18 K range. These spikes are due to physisorbed H_2 which is desorbed from the beam screen's surface. Before summer, this issue was fully understood and solved by cryogenic experts by optimising the cooling loops.

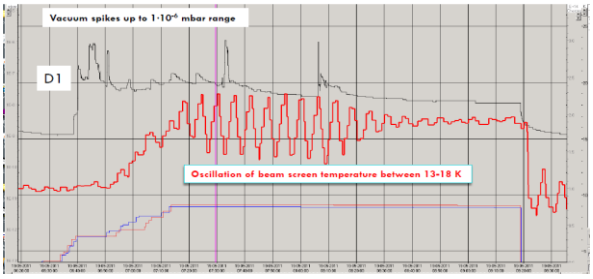

Figure 6: Example of vacuum transient due to beam screen's temperature.

During operation, the condensation of gas onto the beam screen changes also the surface properties of the material. Particularly, adsorption of gas modifies the δ_{max} of the beam screen surface. As an example, Figure 7 shows the effect of condensed CO_2 on as received copper [18]. It is shown that for several monolayers, δ_{max} is well above 1.5 *i.e.* above the multipacting thresholds of Table 2. Obviously, 25 ns beams are more sensitive to physisorbed gas than 50 ns beams.

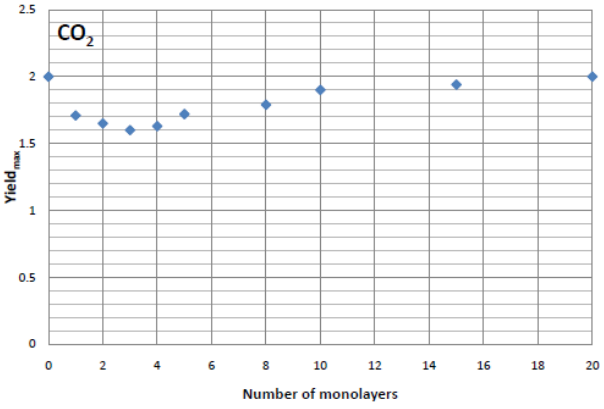

Figure 7: Variation of δ_{max} with the condensation of CO_2 onto as received copper.

For the above reasons, the minimisation of the gas surface coverage onto the beam screen is a must.

It is worth recalling here the LHC vacuum system baseline for the operation with beam screens [19,20]:

- During the cool down of a cryogenic system, the cold bore must be cooled down first and the beam screen afterwards. This procedure keeps the surface coverage of the beam screen as bare as possible.
- Beam screen cooling loops must be optimised in order to avoid transients. Particularly, the beam screen temperature must be kept below 20 K. This procedure allows avoiding crossing adsorption isosteres which generate gas desorption.
- Flushing of the gas from the beam screen to the cold bore by appropriate warm up above 90 K must be done when a lot of gas is accumulated onto the beam screen *e.g.* after scrubbing run, quench etc.
- External evacuation of the condensed gas during technical stops while the cold system is warmed up, allows a definitive removal of the gas from the vacuum system and must be achieved when possible.

UNEXPECTED PRESSURE RISES

By July, till the end of the proton run, pressure spikes were regularly observed during LHC fills while ramping in energy and/or while being in stable beams. These spikes were concentrated in LSS2 and LSS8 beside D1 magnets. X-ray investigations made in autumn revealed that the origin was at the level of the vacuum modules (VAMTF=VMTSA module equipped with VPIA). Previous X-ray imaging done in May'11 indicated that these modules were conform. The sequence of events is not known. Definitely, the heat-induced damage to the spring, which maintains the electrical contact between the RF fingers and the copper insert, is an important issue. This effect is enhanced during the intensity and energy ramp up since the bunch lengths are shortened for few minutes. As a result, the spring left his position leading to a large opening of the RF bridge opening the way to further heating and sparks. Figure 8 shows a typical example of pressure spikes observed during such events, pressure rose up to 10^{-6} mbar. The maximum of the pressure rise is observed at the ion pump (VPIA) exactly at the position of the warm VAMTF modules.

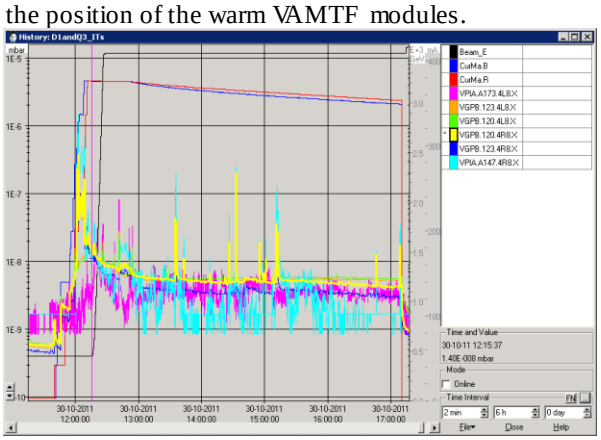

Figure 8: Typical pressure spikes observed in LSS 2 and LSS 8 induced by sparking inside VAMTF module (fill 2267).

During the winter technical stop 2011-12, the 4 vacuum sectors containing VMTSA modules were opened for consolidations (A4L2, A4R2, A4L8 and A4R8). The RF bridges of the module were consolidated. A reinforcement sleeve was installed around the RF fingers, bending the RF fingers towards the insert increased the contact between the fingers and the insert. Ferrites were also installed inside the modules [21]. These ferrites were fully validated in the vacuum laboratory before installation in the machine. The impedance experts validated the consolidated vacuum module. Figure 9 shows the RF

fingers, the reinforcement sleeve and the copper insert. The ferrites to be installed on the left side of the picture are missing.

Figure 9: View of the VMTSA RF bridge. From left to right, reinforcement sleeve, RF finger and copper insert.

Unexpected pressure excursions were also observed in the right side of CMS at 18 m from the interaction point (IP). For a few fills (e.g. fill 2208, 2241), the pressure reached 10^{-6} mbar and slowly decreased in a few hours towards 10^{-8} mbar which completely stopped the CMS data acquisition. Data acquisition could only be resumed when the pressure dropped below 10^{-8} mbar. Figure 10 shows a typical observation made during fill 2160. The orange curve depicted the pressure reading at -18 m. Note that the pressure signal is different from Figure 8. The light green curve depicted the pressure at +18 m. Due to the outgassing of hydrocarbons at -18 mm which are not pumped by the NEG, a similar pressure shape is observed all along CMS.

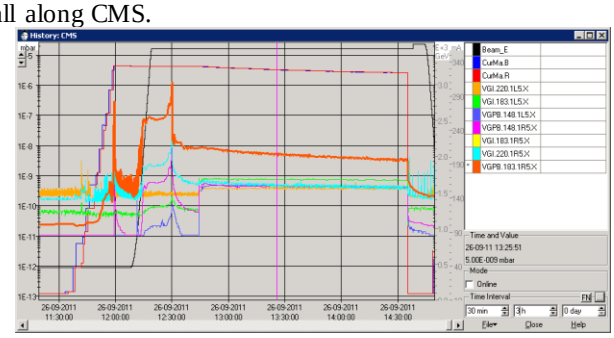

Figure 10: Typical pressure excursion observed only of the right side of CMS (fill 2160).

During Christmas break 2011-2012 when CMS was accessible, X-rays were performed at -18 m as shown by Figure 11. It was found that the RF fingers were inside the copper insert instead of being outside. Probably, the poor contact between the RF fingers and the copper insert induced thermal outgassing and sparking. *In-situ* inspection revealed that the length of the vacuum module was about ~10 mm longer than foreseen. Today, the current understanding of this non-conformity is due to a wrong longitudinal positioning of the TAS 56. The TAS certainly moved between the LHC installation and 2011. Experts are investigating the sequence of events.

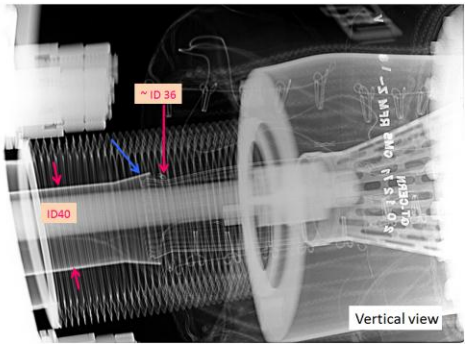

Figure 11: X-ray taken at CMS, 18 m right from the IP. The blue arrow shows the position of the RF fingers which are inside the copper insert [22].

To avoid the risk of aperture restriction by RF fingers, a repair under neon (Ne) atmosphere was done. This method avoided the full bakeout of the CMS vacuum sector which would have meant dismounting the central detector! The CMS vacuum sector was over pressurised by 200 mbar to minimise air back streaming into the NEG coated chambers. Then, the CMS forward chamber was disconnected and moved away to give access to the damaged RF fingers. Then, the replacement assembly was inserted, the CMS forward chamber installed back in place and bolted. The Ne gas used for the venting was evacuated by a mobile pumping group located at Q1R5 to avoid the passage of air-polluted gas through the IP. A pressure of 10^{-9} mbar was reached after 2 days of pumping thereby indicating that the NEG chambers were still pumping. Then, the CMS forward chamber together with the chambers located upstream and downstream to it were re-baked and re-activated. At the end of the intervention, X-ray imaging confirmed the correct positioning of the RF fingers after completing the intervention. The achieved pressures in the vacuum sector were below 10^{-10} mbar and hydrogen transmission measurements through the IP confirmed that the NEG coated vacuum chambers were still activated.

RECOMMENDATIONS AND PERSPECTIVES

During the Christmas break 2011-12, the active cooling of the beam screens was stopped while the cold bore temperatures were kept below 60 K. In the meantime, the beam vacuum system of all the Inner Triplets was evacuated to ensure a permanent removal of potentially harmful physisorbed gas. The cryogenic experts applied the appropriate sequence of cold down of the cold bores / beam screens followed by a temperature conditioning of the beam screens. By these means, the vacuum conditions reached in 2011 are restored.

In parallel, several vacuum sectors were vented for hardware repairs and consolidations (A5L1.B, E5L4.R, D5L4.B, A4L2.C, A4R2.C, A4L8.C and A4R8.C). The NEG coatings of all these vacuum sectors were re-activated and the exposure to the tunnel air was minimised. Figure 12 compares the electron dose required

to scrub an as-received copper surface with the electron dose required to scrub a pre-scrubbed copper surface [23]. The degradation observed after 10 days of air exposure of a previously scrubbed copper surface is marginal. Indeed, the required electron dose to reduce the δ_{max} below the 50 ns threshold is 10 times less than for as received surface. Therefore, the impact of the consolidations done during last Christmas break on the vacuum condition should be negligible.

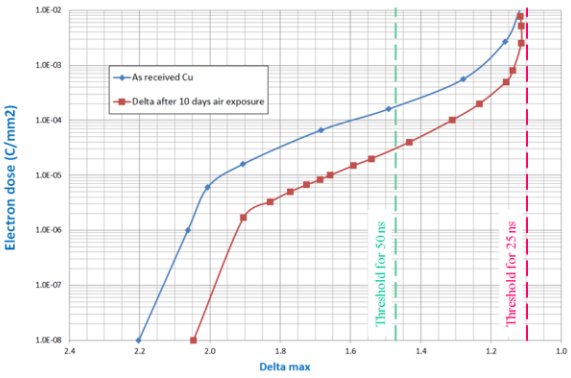

Figure 12: Comparison of scrubbing efficiency between as received and pre-scrubbed copper.

However, for the upgrade of the ZDC detector, ~5 m of new vacuum chambers (ID800 mm) were installed [24]. As agreed with the representative of ALICE experiment, this upgrade will temporarily affect the vacuum performances of the vacuum sectors A4L2.C and A4R2.C which could worsen the background to the ALICE experiment. Moreover, during 2011 run, pressure rise in the range 10^{-8} mbar were observed along the ID800 vacuum chambers (~15 m long). The behaviour of this pressure rise was typical of electron cloud as confirmed by simulations [25,26]. Therefore, during 2012, more scrubbing is required to scrub the new vacuum chambers but also to reduce further the pressure rise observed in the ID800 vacuum chambers. Obviously, operating with 25 ns beam would help to reduce further the pressure levels in these vacuum sectors.

In 2012, the operation with 50 ns with an immediate start up to 1.45 10^{11} ppb should be possible while scrubbing the vacuum system in the shadow of the intensity ramp up. However, an immediate start up to 1.6 10^{11} ppb will require a couple of days of scrubbing with 25 ns beams. Physics operation with 25 ns beams will require a dedicated scrubbing run at 25 ns with the objective to reach the LHC design parameters.

CONCLUSIONS

With the increase of the LHC performance towards the nominal parameters, dynamic pressure rises were observed, as expected, in the LHC vacuum system. Photon stimulated molecular desorption induced by SR was observed in the LHC arcs as well as in separation dipoles. The pressure reductions observed during beam conditioning are in agreements with published data. Electron stimulated molecular desorption induced by the electron cloud was also observed in the entire ring, with the exception of the NEG coated vacuum chambers, as expected. A scrubbing run together with the continuous scrub while operating in physics, reduced the δ_{max} to 1.4 and 1.5 in the uncoated straight sections and in the arcs respectively [4]. A pressure reduction of more than one order of magnitude was observed during the year whilst pushing the LHC performances to their limits.

All unexpected pressures behaviours observed during 2011 are understood. Most of the issues were addressed and fixed or consolidated during the Christmas break 2011-12. The remaining issues will be fixed during the next long shutdown while consolidating the LHC vacuum system [27].

ACKNOWLEDGEMENTS

The authors would like to thanks the engineers and charge and operators with the equipment owners for their proactive feedbacks in such a way to maintain the vacuum performances. The authors would like also to warmly acknowledge P. Chiggiato and P. Cruikshank for their interest and participation to the scrubbing runs and machine developments periods related to electron cloud. Finally, the VSC group management would like to thanks all the group members and particularly the members of the LBV section for their strong commitment during the LHC operation, technical stops and Christmas breaks.

REFERENCES

[1] Overview of the LHC Vacuum System. O. Gröbner, Vacuum 60 (2001) 25-34.
[2] LHC design report. CERN-2004-003
[3] Molecular Desorption by Synchrotron Radiation and sticking coefficient at cryogenic temperatures for H_2, CH_4, CO and CO_2. V. Baglin *et al*. Vacuum 67 (2002) 421-428.
[4] LHC Experience with Different Bunch Spacings in 2011 (25, 50 & 75 ns). G. Rumolo *et al*. Proceedings of Chamonix 2012.
[5] Electron Cloud and Beam Scrubbing in the LHC. N. Hilleret *et al*. Proceedings of PAC-99, New York, 1999.
[6] Ion Induced Gas Desorption problem in the ISR. R. Calder, Vacuum 24-10 (1974) 437-443.
[7] Ion Desorption Vacuum Stability in the LHC the Multigas Model. O. Malyshev *et al*. Proceedings of EPAC 2000, Vienna, 2000.
[8] Vacuum Calculations for the LHC Experimental Beam Chambers. A. Rossi *et al*. Proceedings of PAC 2001, Chicago, 2001.
[9] Synchrotron Radiation in the LHC Vacuum system. V. Baglin *et al*. Proceedings of IPAC 2011, San Sebastian, 2011.
[10] Dynamic Outgassing. O. Gröbner, CERN Accelerator School, CERN 99-05, Snekersten, 1999.

[11] Vacuum and Cryogenic Observations for Different Bunch Spacing. J.M Jimenez *et al*. Proceedings of Chamonix 2011.
[12] Observations of electron Cloud Effects in the LHC Vacuum System. G. Bregliozzi *et al*. Proceedings of IPAC 2011, San Sebastian, 2011.
[13] Vacuum Pressure Observations During 2011 Proton Run. G. Bregliozzi *et al*. Proceedings of Evian 2011.
[14] LHC Scrubbing Run April 2011: Cryogenic Observations in the Arcs. L. Tavian. LHC Beam Operation Committee, 12/4/2011, CERN, 2011.
[15] A Summary of Main Experimental Results Concerning the Secondary Electron Emission of Copper. N. Hilleret *et al*. LHC Project Report 472, CERN, 2001.
[16] Some Observations During the 25 ns MD done on 24-25/10/2011. E. Metral *et al*. 112th LHC Machine Committee, CERN, 2011.
[17] Vacuum Transients during LHC Operation. V. Baglin. Proceedings of LHC Project Workshop – Chamonix XIII, Chamonix, 2004.
[18] Secondary Electron Yield on Cryogenic Surfaces as a Function of Physisorbed Gases. A. Kuzucan. PhD thesis, Vienna University, 2011.
[19] Beam Screens for the LHC Arc Magnets. N. Kos *et al*. LHC-VSS-ES-0001.00 rev. 1.0, edms 107716, 2001.
[20] Beam Screens for the LHC Long Straight Sections. N. Kos *et al*. LHC-VSS-ES-0002 rev. 1.3, edms 334961, 2007.
[21] Modification of VMTSA RF fingers. V. Baglin. LHC-VMTSA-EC-0001 ver. 0.1, edms 117900, 2012.
[22] X-rays image taken the 21st December 2011. J-M. Dalin *et al*, CERN EN-MME.
[23] Electron Cloud with LHC-Type Beams in the SPS: a Review of Three Years of Measurements. J.M Jimenez *et al*. LHC Project Report 623, CERN, 2003.
[24] Modification IR2 to solve the ALICE ZDC-TCTVB Interference Problem. D. Macina, N. De Marco. LHC-LJ-EC-0025 ver. 1.0, edms 1153295, 2011.
[25] Vacuum Observations. G. Bregliozzi. LHC Beam Operation Committee, 27/7/2011, CERN, 2011.
[26] G. Rumolo, G. Iadarola, Private Communications January 2012.
[27] LHC Upgrade During LS1. J.M. Jimenez *et al*. Proceedings of Chamonix 2012.